

# Accepted Manuscript

Ultrastructural changes of the vitreoretinal interface during long-term follow-up after removal of the internal limiting membrane

Toshio Hisatomi , Shoji Notomi , Takashi Tachibana , Yukio Sassa , Yasuhiro Ikeda , Takao Nakamura , Akifumi Ueno , Hiroshi Enaida , Toshinori Murata , Taiji Sakamoto , Tatsuro Ishibashi

PII: S0002-9394(14)00293-1

DOI: [10.1016/j.ajo.2014.05.022](https://doi.org/10.1016/j.ajo.2014.05.022)

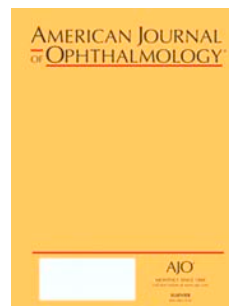
Reference: AJOPHT 8928

To appear in: *American Journal of Ophthalmology*

Received Date: 11 April 2014

Revised Date: 16 May 2014

Accepted Date: 16 May 2014



Please cite this article as: Hisatomi T, Notomi S, Tachibana T, Sassa Y, Ikeda Y, Nakamura T, Ueno A, Enaida H, Murata T, Sakamoto T, Ishibashi T, Ultrastructural changes of the vitreoretinal interface during long-term follow-up after removal of the internal limiting membrane, *American Journal of Ophthalmology* (2014), doi: 10.1016/j.ajo.2014.05.022.

This is a PDF file of an unedited manuscript that has been accepted for publication. As a service to our customers we are providing this early version of the manuscript. The manuscript will undergo copyediting, typesetting, and review of the resulting proof before it is published in its final form. Please note that during the production process errors may be discovered which could affect the content, and all legal disclaimers that apply to the journal pertain.

## Abstract

Purpose: In order to investigate long-term ultrastructural changes in the retina after internal limiting membrane (ILM) peeling, we examined morphological changes three years after vitrectomy in cynomolgus monkeys.

Design: Laboratory investigation.

Methods: Pars plana vitrectomy was performed followed by ILM peeling in two primate eyes. Ultrastructural changes were investigated using light microscopy and, transmission and scanning electron microscopy three years after ILM peeling.

Results: The remaining posterior vitreous and ILM peeled areas were clearly recognized after the long-term follow-up. The exposed Müller cell processes were partially damaged, while regenerative spindle-shaped Müller cell processes developed, covering most of the retina. Notably, the nerve fiber layer was found to be uncovered and exposed to the vitreous space due to misdirection of glial wound healing in some parts. In these areas, glial wound healing occurred beneath the nerve fiber layer.

Although the glial cells covered the damaged areas, there was no apparent ILM regeneration in the shape of a continuous flat sheet, with the exception of accumulated deposits of basement membrane materials.

Conclusions: Although the retinal structures were well preserved after ILM peeling, ILM peeling resulted in mild damage to the vitreoretinal interface, which was not completely restored even after three years. The multi-linear shape of the exposed nerve fiber may explain the previously reported dissociated optic nerve fiber layer appearance. The glial cells produced basement membrane materials around their processes, although they did not restore the ILM as a flat sheet.

Ultrastructural changes of the vitreoretinal interface during long-term follow-up after removal of the internal limiting membrane.

Toshio Hisatomi,<sup>1,2</sup> Shoji Notomi,<sup>1,2</sup> Takashi Tachibana,<sup>1</sup> Yukio Sassa,<sup>1</sup> Yasuhiro Ikeda,<sup>1</sup> Takao Nakamura,<sup>1</sup> Akifumi Ueno,<sup>1</sup> Hiroshi Enaida,<sup>1</sup> Toshinori Murata,<sup>1</sup> Taiji Sakamoto,<sup>3</sup> Tatsuro Ishibashi<sup>1</sup>

<sup>1</sup>Department of Ophthalmology, Graduate School of Medical Sciences, Kyushu University, 3-1-1 Maidashi Higashi-ku, Fukuoka, 812-8582, Japan, <sup>2</sup>Clinical Research Institute, Kyushu Medical Centre, 1-8-1 Jigyo-Hama chuo-ku, Fukuoka, Japan,

<sup>3</sup>Department of Ophthalmology, Kagoshima University School of Medicine, 8-35-1 Sakuragaoka, Kagoshima, 890-8520, Japan

(Current location) Nakamura eye clinic, 1-5-3 Shirakibaru, Onojyo, Japan (TN), Oshima eye hospital, 11-8 Kamigofukumachi Hakata-ku, Fukuoka, Japan (AU), Department of Ophthalmology, Saga University School of Medicine, 5-1-1 Nabeshima, Saga, 849-8501, Japan (HE), Shinshu University School of Medicine, 3-1-1 Asahi, Matsumoto, Nagano 390-8621, Japan (TM).

Short running title: Ultrastructure after internal limiting membrane peeling.

Correspondence and reprint requests should be addressed to: Toshio Hisatomi MD, PhD, Department of Ophthalmology, Graduate School of Medical Sciences, Kyushu University, 3-1-1 Maidashi, Higashi-ku, Fukuoka, 812-8582, Japan, TEL +81-92-642-5648, FAX +81-92-642-5663, E-Mail [hisatomi@med.kyushu-u.ac.jp](mailto:hisatomi@med.kyushu-u.ac.jp)

Key words:

Vitrectomy, internal limiting membrane (ILM), epiretinal membrane (ERM), Müller cell, dissociated optic nerve fiber layer, brilliant blue G

## Introduction

The pathogenesis of various vitreoretinal diseases is still not fully understood. However, there is agreement regarding the important role of vitreous attachment and vitreous traction to the underlying internal limiting membrane (ILM) and retina. The ILM is originally produced by Müller glial cells during the development of the retina and provides basement membrane under normal conditions or extracellular matrix for cellular migration and contraction under pathological conditions. Histological examinations of excised ILMs have demonstrated that migrating cells of various origins are located on the ILM and that these cells are associated with collagen fibers of various diameters<sup>1-5</sup>. ILM peeling during vitrectomy drastically increases the closure rate in macular holes<sup>6-9</sup>. ILM peeling allows for the complete removal of the posterior vitreous cortex, contraction of the extracellular matrix and cellular migration. In addition, ILM peeling has been widely performed to treat patients with vision-threatening vitreoretinal diseases, such as severe myopic retinal detachment or proliferative vitreoretinopathy<sup>10, 11</sup>.

However, there has been some concern regarding the adverse effects of this technique since the ILM constitutes the basement membrane of Müller cells and the inner barrier of the neural retina. In our previous report, damaged underlying Müller cell processes were observed just beneath the ILM immediately after ILM peeling<sup>12</sup>. In some areas, glial cell processes laying between the ILM and nerve fiber layer were removed. Consequently, the nerve fibers were exposed directly to the vitreous space without glial cells. Although we previously reported the early morphological changes observed after experimental ILM peeling in cynomolgus monkeys, the long-term outcomes after ILM peeling remain elusive. Although morphological changes after ILM peeling have been observed under optical coherence tomography (OCT), the correlations between OCT findings and pathological changes are clinically important. The irregular appearance of the retina after ILM peeling surgery in the fundus or OCT examinations may reflect pathological changes. In this report, we evaluated ultrastructural changes and remodeling of the retina three years after experimental vitrectomy with ILM peeling.

## METHODS

### Animals

The study was designed as a laboratory investigation. All experiments were performed in accordance with the Association for Research in Vision and Ophthalmology (ARVO) Statement for the Use of Animals in Ophthalmic and Vision Research and approved by the animal care and use committee at Kyushu University, Fukuoka, Japan. Two eyes from two cynomolgus monkeys between 3 and 4 years of age were used in this experiment. The cynomolgus monkeys were restrained in a squeeze cage and injected intramuscularly in the thigh with 20 mg/kg of ketamine hydrochloride (Sankyo Yell Pharmaceutical Products Co., Ltd., Japan) for general anesthesia. The monkeys were subsequently transported to the operating room.

### Vitrectomy and internal limiting membrane peeling

Standard three-port pars plana vitrectomy and ILM peeling were performed in a closely similar fashion to that carried out in human patients, as previously reported<sup>12</sup>. The internal limiting membrane was stained a light green color with 0.5% indocyanine green (ICG) solution<sup>12</sup>. The internal limiting membrane was removed in a circular fashion up to the temporal arcade and optic disc. The instruments were then removed and the sclerotomy ports were closed using 7-0 polygalatin sutures.

The monkeys were euthanized with an overdose of sodium pentobarbital (200mg/kg) and the eyes were enucleated three years (n=2) after surgery. The enucleated eyes were fixed with 1 % glutaraldehyde and 2 % osmium tetroxide. The posterior parts of the eyes were prepared under a biomicroscope (Nikon, Tokyo) for the histopathological analyses.

### Transmission electron microscopy

The posterior segments were fixed in 1% glutaraldehyde and 1% paraformaldehyde in PBS. The retinas were postfixed in veronal acetate buffer osmium tetroxide (2%), dehydrated in a series of ethanol and water, and embedded in Epon. Semi-thin sections were cut from block and observed under a light microscope (Olympus, Tokyo). Ultrathin sections were mounted on copper grids and observed with a JEM 100CX (JEOL, Tokyo), H-7650 and H-7700 electron microscope (Hitachi, Tokyo)<sup>13-16</sup>.

### Scanning electron microscopy

The retinas were post-fixed in veronal acetate buffer osmium tetroxide (2%), and dehydrated in ethanol and water. The retinas were saturated in t-butyl alcohol, and critical point drying was performed. The tissue was then placed on stubs by means of self-adhering carbon tabs and sputtered with Au of 20nm in thickness using an argon plasma coater. Then retinal surface of the eyes was then studied under a scanning electron microscope (JSM-840A)<sup>4, 5, 15, 17</sup>.

## RESULTS

### Biomicroscopy and light microscopy

The fixed eyes were cut and the posterior part was observed under a biomicroscope (Figure 1). The eyecup showed a well-preserved structure in the posterior portion of the monkey eye, similar to that observed in the human eye (Figure 1, top left). While the optic disc and macula were clearly recognized, the area with ILM peeling was not obvious under wet conditions (Figure 1, top left). The sample preparation using critical point drying minimized ultrastructural changes for successful scanning electron microscopy (Figure 1, top right). Under dry conditions, the artificial posterior vitreous detachment and remaining posterior vitreous were clearly observed around the posterior part of the eyes. Light microscopic images of semi-thin sections showed well-preserved structures of the retina in the ILM-peeled areas compared to that noted in the neighboring normal retina. The retinal thickness of the ILM-peeled areas was similar to that of the normal areas (Figure 1, bottom left and right).

### Scanning electron microscopy

The low-magnification images provided a bird's eye view of the posterior parts of the eye and the major structures, such as the remaining posterior vitreous, ILM, macula and optic disc (Figure 2, top). The remaining posterior vitreous was rolled up on the vitreous surface (Figure 2, middle left). The normal area without ILM peeling was observed as a dark area on the retina, while the lighter area that surrounds the foveal pit is the zone of ILM detachment. The retina with ILM peeling exhibited an irregular surface structure with cellular components compared to smooth flat surface structure of the normal retina (Figure 2, top). Most parts of the retina with ILM peeling were covered with Müller cell processes, whereas glial cell processes reproduced the flattened surface of the retina (Figure 2, middle right). In some parts, multi-linear wave fibrillary structures considered to be denuded nerve fibers were observed without covering Müller cell processes (Figure 2, bottom left and right, arrows). The denuded nerve fibers created a rough retinal surface without glial processes. There was no apparent ILM regeneration as a flat sheet covering the ILM-peeled retina.

### Transmission electron microscopy

The regenerative Müller cell processes extended and covered the wounded areas with ILM peeling (Figure 3, top). The abundant intermediate filaments in the cytoplasm of these cells indicated that these cells were Müller glial cells. The surface of the exposed retina was covered with densely packed, multi-layered Müller cell processes (Figure 3, middle left). In some areas, the nerve fiber layer was uncovered and exposed to the vitreous space due to misdirection of glial wound healing (Figure 3, middle right). The glial wound healing developed beneath the nerve fiber layer or shaped the Müller cell wound cleft (Figure 3, middle right and bottom left). In the Müller cell wound cleft, glial cells left some spaces among the cellular endfeet, and basement materials had accumulated in the spaces (Figure 3, bottom left). Although the glial cells covered the damaged areas, there was no apparent ILM regeneration as a continuous flat sheet, with the exception of accumulated deposits of basement membrane materials around the Müller cell processes (Figure 3, bottom left and right).

## DISCUSSION

In this study, we reported novel findings regarding ultrastructural changes on vitreoretinal interface three years after experimental vitrectomy with ILM peeling. Glial cell remodeling and wound healing process successfully covered most part of the areas damaged by ILM peeling. Notably, the nerve fiber layer was found to be uncovered and exposed to the vitreous space, even after three years, due to misdirection of glial wound healing in some parts. In these areas, glial wound healing occurred beneath the nerve fiber layer or shaped the Müller cell wound cleft. Although the glial cells covered the damaged areas, no apparent vitreous or ILM regeneration was detected in the specimens.

The ILM is originally produced by Müller glial cells during the development of the eyes. Since glial cells produce and secrete basement membrane materials, we had expected that ILM regeneration would be observed as a continuous flat sheet after the long observation period of three years<sup>12</sup>. However, we found no regenerated continuous flat sheets, with the exception of accumulated deposits of basement membrane materials in the Müller cell wound cleft or on retinal surface glial processes (Figure 3). These findings indicate that the glial cells still continued to produce and secrete basement membrane materials. The materials were observed in limited spaces surrounded by Müller cells.

There are two potential factors leading to retinal damage in the setting of ICG-assisted ILM peeling: the toxicity of ICG used for chromovitrectomy, and the mechanical damage caused by ILM peeling itself. As we have previously reported the potential adverse effects of ICG<sup>18-20</sup>, we searched for suitable dyes allowing for better visualization and biocompatibility than other reported dyes and finally assessed brilliant blue G using basic and clinical trials<sup>21-23</sup>. Brilliant blue G is now used for chromovitrectomy<sup>24, 25</sup>. We also reported the neuroprotective effects of brilliant blue G achieved via the blockade of the proapoptotic cellular surface purinergic receptor P2X, ligand-gated ion channel, 7<sup>26-30</sup>. In addition, the fragments of the Müller cells detected on excised ILM samples indicate that ILM peeling may damage the inner part of the retina<sup>12, 31</sup>. Müller cells extend their processes throughout the retina to contact with and ensheathe every type of neural cell body and axon. In the present study, during the

wound healing that occurred over three years, the Müller processes successfully covered most parts of ILM peeling areas (Figure 2 bottom left, 3 top) but failed to ensheathe nerve fibers in some areas. The uncovered nerve fibers, namely ganglion cell axons, appeared to exhibit a normal cellular activity (Figure 3, middle right), partly due to support by misdirected glial processes beneath the nerve fiber layer. Tadayoni reported the presence of arcuate striae in the direction of optic nerve fibers after vitrectomy as dissociated optic nerve fiber layer appearance<sup>32</sup>. The multi-linear shape of the exposed nerve fiber may resemble and explain the reported dissociated optic nerve fiber layer appearance. A dissociated optic nerve fiber layer appearance is not associated with postoperative visual acuity, visual field, or electroretinogram findings<sup>33-35</sup>. In the current study, the exposed nerve fiber remained uncovered without Müller cell processes; however, the retinal structures and thickness were preserved in the ILM-peeled areas, in line with dissociated optic nerve fiber layer reports. Considering our results, a dissociated optic nerve fiber layer appearance may also include a “denuded optic nerve fiber layer” in addition to a dissociated nerve fiber layer. Further studies are needed to clarify the pathological and functional aspects of potential damage and wound healing after ILM peeling.

Performing careful surgical procedures is important for minimizing potential damage and obtaining better surgical outcomes with vitrectomy. Further studies may increase understanding of the vitreoretinal interface in patients with retinal pathology and improve future surgical techniques.

**Acknowledgments/disclosure**

- a. Funding/Support: Funding: A Grant-in-Aid for Scientific Research from the Ministry of Education, Science, and Culture of the Japanese Government (Tokyo, Japan)
- b. Financial Disclosures: Consultancy from Bausch and Lomb (Tokyo, Japan), Wakamoto Co., Ltd. (Tokyo, Japan), (TI), Grants from Santen Pharm Co., Ltd.(Osaka, Japan), Novartis K.K. (Tokyo, Japan), Wakamoto Co.,Ltd, Pfizer Japan, Inc. (Tokyo, Japan), Senju Pharm Co., Ltd. (Osaka, Japan), Hoya Corp. (Tokyo, Japan), Kowa Co., Ltd. (Nagoya, Japan), (TI), Payment for lectures from Santen Pharm Co., Ltd., Novartis K.K., Pfizer Japan, Inc, Senju Pharm Co., Ltd, Kowa Co., Ltd. (TI), and Travel/accommodations/meeting expenses from Santen Pharm Co., Ltd., Novartis K.K., Pfizer Japan, Inc, Senju Pharm Co., Ltd, Alcon Japan. Ltd. (Tokyo, Japan), Kowa Co., Ltd. (TI).
- c. Contributions of the authors: design and conduct of the study (TH, SN, TT, YS, YI, TN, AU, HE); collection, management, analysis, and interpretation of the data (TH, SN, TT, YS, YI, TN, AU, HE, TM, TS); preparation, review, and/or approval of the manuscript (TH, TM, TS, TI).
- d. Other Acknowledgments: none.

## References

1. Kampik A, Green WR, Michels RG, Nase PK. Ultrastructural features of progressive idiopathic epiretinal membrane removed by vitreous surgery. *Am J Ophthalmol* 1980;90(6):797-809.
2. Smiddy WE, Michels RG, de Bustros S, de la Cruz Z, Green WR. Histopathology of tissue removed during vitrectomy for impending idiopathic macular holes. *Am J Ophthalmol* 1989;108(4):360-364.
3. Messmer EM, Heidenkummer HP, Kampik A. Ultrastructure of epiretinal membranes associated with macular holes. *Graefes Arch Clin Exp Ophthalmol* 1998;236(4):248-254.
4. Hisatomi T, Enaida H, Sakamoto T, et al. A new method for comprehensive bird's-eye analysis of the surgically excised internal limiting membrane. *Am J Ophthalmol* 2005;139(6):1121-1122.
5. Hisatomi T, Enaida H, Sakamoto T, et al. Cellular migration associated with macular hole: a new method for comprehensive bird's-eye analysis of the internal limiting membrane. *Arch Ophthalmol* 2006;124(7):1005-1011.
6. Eckardt C, Eckardt U, Groos S, Luciano L, Reale E. [Removal of the internal limiting membrane in macular holes. Clinical and morphological findings]. *Ophthalmologe* 1997;94(8):545-551.
7. Park DW, Sipperley JO, Snead SR, Dugel PU, Jacobsen J. Macular hole surgery with internal-limiting membrane peeling and intravitreous air. *Ophthalmology* 1999;106(7):1392-1397.
8. Kadonosono K, Itoh N, Uchio E, Nakamura S, Ohno S. Staining of internal limiting membrane in macular hole surgery. *Arch Ophthalmol* 2000;118(8):1116-1118.
9. Burk SE, Da Mata AP, Snyder ME, Rosa RH, Jr., Foster RE. Indocyanine green-assisted peeling of the retinal internal limiting membrane. *Ophthalmology* 2000;107(11):2010-2014.
10. Kadonosono K, Yazama F, Itoh N, et al. Treatment of retinal detachment resulting from myopic macular hole with internal limiting membrane removal. *Am J Ophthalmol* 2001;131(2):203-207.

11. Kusaka S, Hayashi N, Ohji M, Hayashi A, Kamei M, Tano Y. Indocyanine green facilitates removal of epiretinal and internal limiting membranes in myopic eyes with retinal detachment. *American Journal of Ophthalmology* 2001;131(3):388-390.
12. Nakamura T, Murata T, Hisatomi T, et al. Ultrastructure of the vitreoretinal interface following the removal of the internal limiting membrane using indocyanine green. *Curr Eye Res* 2003;27(6):395-399.
13. Hisatomi T, Sakamoto T, Murata T, et al. Relocalization of apoptosis-inducing factor in photoreceptor apoptosis induced by retinal detachment in vivo. *Am J Pathol* 2001;158(4):1271-1278.
14. Hisatomi T, Sakamoto T, Goto Y, et al. Critical role of photoreceptor apoptosis in functional damage after retinal detachment. *Curr Eye Res* 2002;24(3):161-172.
15. Hisatomi T, Sakamoto T, Sonoda KH, et al. Clearance of apoptotic photoreceptors: elimination of apoptotic debris into the subretinal space and macrophage-mediated phagocytosis via phosphatidylserine receptor and integrin alphavbeta3. *Am J Pathol* 2003;162(6):1869-1879.
16. Hisatomi T, Sonoda KH, Ishikawa F, et al. Identification of resident and inflammatory bone marrow derived cells in the sclera by bone marrow and haematopoietic stem cell transplantation. *Br J Ophthalmol* 2007;91(4):520-526.
17. Matsumoto H, Yamanaka I, Hisatomi T, et al. Triamcinolone acetonide-assisted pars plana vitrectomy improves residual posterior vitreous hyaloid removal: ultrastructural analysis of the inner limiting membrane. *Retina* 2007;27(2):174-179.
18. Enaida H, Sakamoto T, Hisatomi T, Goto Y, Ishibashi T. Morphological and functional damage of the retina caused by intravitreous indocyanine green in rat eyes. *Graefes Arch Clin Exp Ophthalmol* 2002;240(3):209-213.
19. Kanda S, Uemura A, Yamashita T, Kita H, Yamakiri K, Sakamoto T. Visual field defects after intravitreous administration of indocyanine green in macular hole surgery. *Arch Ophthalmol* 2004;122(10):1447-1451.
20. Kawahara S, Hata Y, Miura M, et al. Intracellular events in retinal glial cells exposed to ICG and BBG. *Invest Ophthalmol Vis Sci* 2007;48(10):4426-4432.

21. Hisatomi T, Enaida H, Matsumoto H, et al. Staining ability and biocompatibility of brilliant blue G: preclinical study of brilliant blue G as an adjunct for capsular staining. *Arch Ophthalmol* 2006;124(4):514-519.
22. Enaida H, Hisatomi T, Goto Y, et al. Preclinical investigation of internal limiting membrane staining and peeling using intravitreal brilliant blue G. *Retina* 2006;26(6):623-630.
23. Enaida H, Hisatomi T, Hata Y, et al. Brilliant blue G selectively stains the internal limiting membrane/brilliant blue G-assisted membrane peeling. *Retina* 2006;26(6):631-636.
24. Shimada H, Nakashizuka H, Hattori T, Mori R, Mizutani Y, Yuzawa M. Double staining with brilliant blue G and double peeling for epiretinal membranes. *Ophthalmology* 2009;116(7):1370-1376.
25. Kadonosono K, Arakawa A, Inoue M, et al. Internal limiting membrane contrast after staining with indocyanine green and brilliant blue G during macular surgery. *Retina* 2013;33(4):812-817.
26. Hisatomi T, Nakazawa T, Noda K, et al. HIV protease inhibitors provide neuroprotection through inhibition of mitochondrial apoptosis in mice. *J Clin Invest* 2008;118(6):2025-2038.
27. Hisatomi T, Ishibashi T, Miller JW, Kroemer G. Pharmacological inhibition of mitochondrial membrane permeabilization for neuroprotection. *Exp Neurol* 2009;218(2):347-352.
28. Notomi S, Hisatomi T, Kanemaru T, et al. Critical involvement of extracellular ATP acting on P2RX7 purinergic receptors in photoreceptor cell death. *Am J Pathol* 2011;179(6):2798-2809. doi: 2710.1016/j.ajpath.2011.2708.2035.
29. Hisatomi T, Nakao S, Murakami Y, et al. The regulatory roles of apoptosis-inducing factor in the formation and regression processes of ocular neovascularization. *Am J Pathol* 2012;181(1):53-61.
30. Notomi S, Hisatomi T, Murakami Y, et al. Dynamic increase in extracellular ATP accelerates photoreceptor cell apoptosis via ligation of P2RX7 in subretinal hemorrhage. *PLoS One* 2013;8(1):e53338.

31. Yooh HS, Brooks HL, Jr., Capone A, Jr., L'Hernault NL, Grossniklaus HE. Ultrastructural features of tissue removed during idiopathic macular hole surgery. *Am J Ophthalmol* 1996;122(1):67-75.
32. Tadayoni R, Paques M, Massin P, Mouki-Benani S, Mikol J, Gaudric A. Dissociated optic nerve fiber layer appearance of the fundus after idiopathic epiretinal membrane removal. *Ophthalmology* 2001;108(12):2279-2283.
33. Mitamura Y, Suzuki T, Kinoshita T, Miyano N, Tashimo A, Ohtsuka K. Optical coherence tomographic findings of dissociated optic nerve fiber layer appearance. *Am J Ophthalmol* 2004;137(6):1155-1156.
34. Mitamura Y, Ohtsuka K. Relationship of dissociated optic nerve fiber layer appearance to internal limiting membrane peeling. *Ophthalmology* 2005;112(10):1766-1770.
35. Kishimoto H, Kusuhara S, Matsumiya W, Nagai T, Negi A. Retinal surface imaging provided by Cirrus high-definition optical coherence tomography prominently visualizes a dissociated optic nerve fiber layer appearance after macular hole surgery. *Int Ophthalmol* 2011;31(5):385-392.

## Figure Legends

### Figure 1

Macroscopic and microscopic images of the vitreoretinal interface during sample preparation. (Top left) The posterior part of the eye was observed under a biomicroscope. (Top right) Critical point drying visualized the posterior vitreous remaining on the retina. (Bottom left) A low-magnification light microscopic image of a semi-thin section. The retinal structures were well preserved in both the normal and internal limiting membrane (ILM) peeled areas. The arrows indicate the edge of the remaining ILM. The retinal thickness is similar in the two areas. (Bottom right) A high-magnification light microscopic image shows preserved cellular components of the retina. (Original magnification top left x2, top right x3, bottom left x100, bottom right x200)

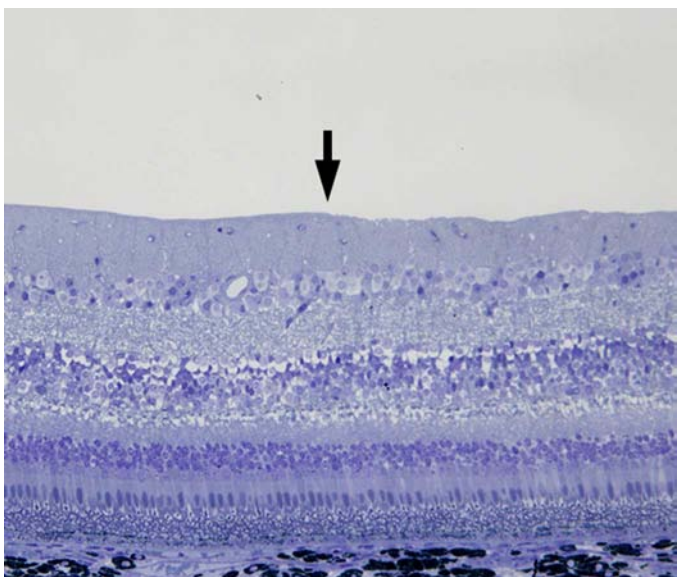
### Figure 2

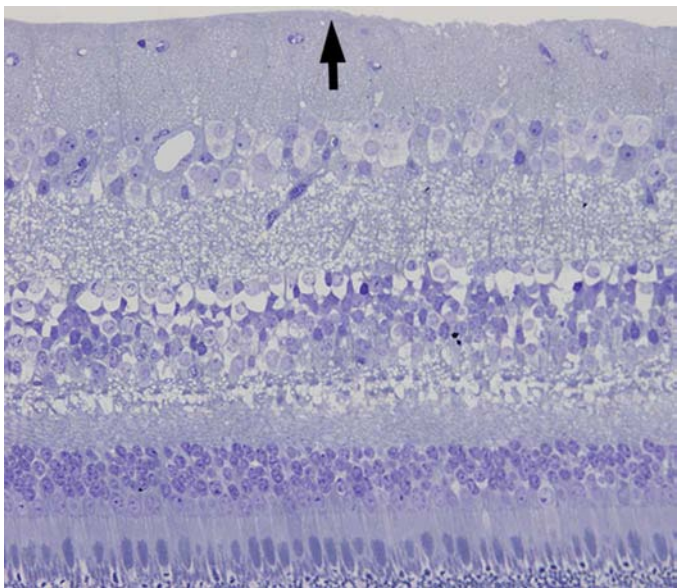
Scanning electron microscopic images of the vitreoretinal interface after internal limiting membrane (ILM) peeling. (Top) A medium-magnification image clearly shows the remaining posterior vitreous and ILM-peeled area on the retina (arrows). A normal area without ILM peeling was observed as a dark area on the retina, the lighter area that surrounds the foveal pit was the zone of ILM detachment. The retina with ILM peeling exhibits an irregular surface structure with cellular components compared to the smooth flat surface structure of the normal retina. (Middle left) The remaining posterior vitreous was rolled up on the vitreous surface. (Middle right) The macula displays a well preserved structure of the fovea and glial processes covering the ILM-peeled area. (Bottom left) A high-magnification image shows glial processes covering most parts of the ILM peeled area. Nerve fibers are noted on the retinal surface (arrow) in some parts. (Bottom right) Denuded nerve fibers demonstrate a multi-linear wave pattern, creating a rough retinal surface. (Original magnification top x20 bar 1mm, middle left x120 bar 100µm, middle right x120 bar 100µm, bottom left x500 bar 10µm, bottom right x3,000 bar 10µm)

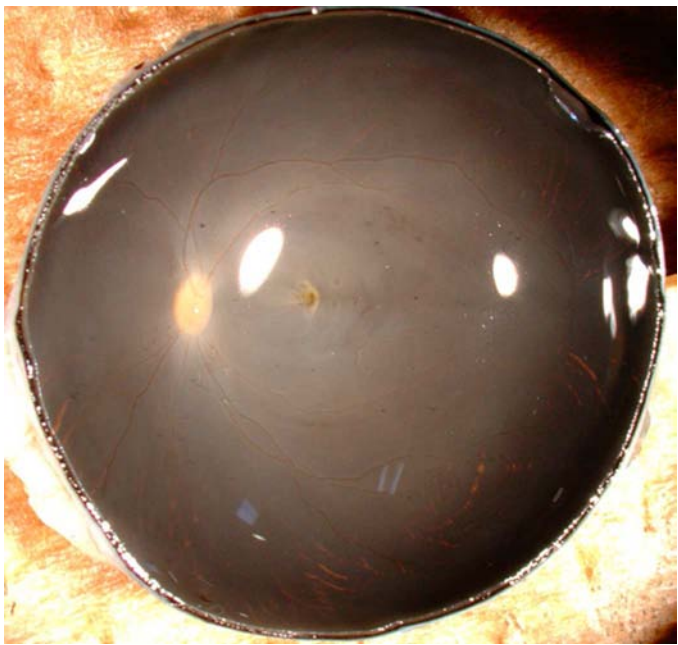
### Figure 3

Transmission electron microscopic images of the vitreoretinal interface after internal

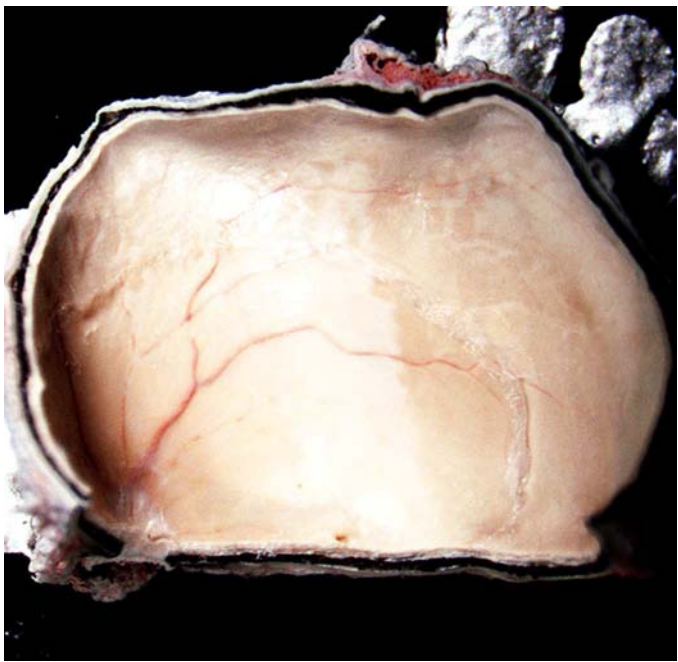
limiting membrane (ILM) peeling. (Top) A low-magnification image clearly shows the edge of the remaining ILM (black arrows). Major structures of the retina, such as Müller cells and the nerve fiber layer (NFL), were well preserved three years after ILM peeling. (Middle left) The edge of ILM was noted, and there was no ILM regeneration as a continuous flat sheet. (Middle right) The nerve fiber is left uncovered without surrounding glial processes in some parts (white arrow). (Bottom left) Basement membrane materials had accumulated in the wound cleft between Müller cells (black arrowheads). (Bottom right) Some basement materials were also detected on the retinal surface covered with glial processes (white arrowheads). (Original magnification top x1,000 bar 5 $\mu$ m, middle left x3,000 bar 1 $\mu$ m, middle right x3,000 bar 1 $\mu$ m, bottom left x2,000 bar 1 $\mu$ m, bottom right x6,000 bar 1 $\mu$ m)



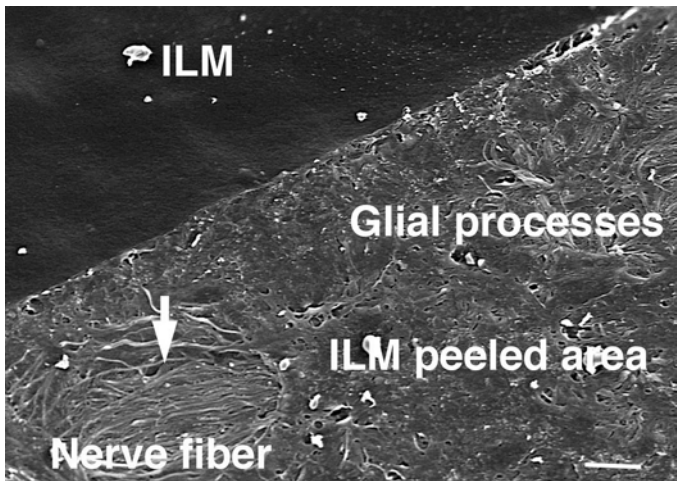


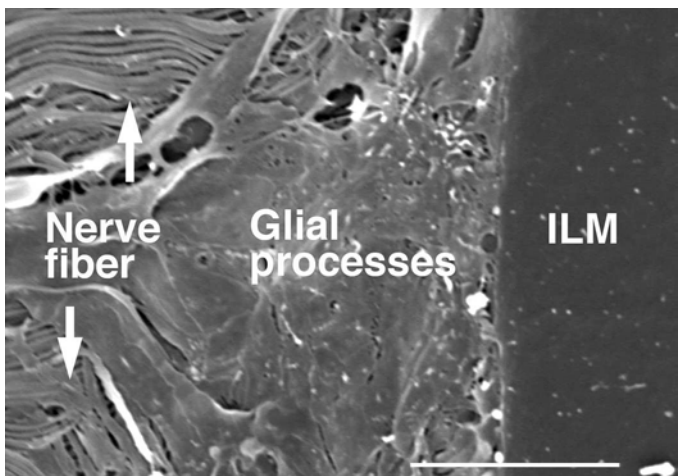


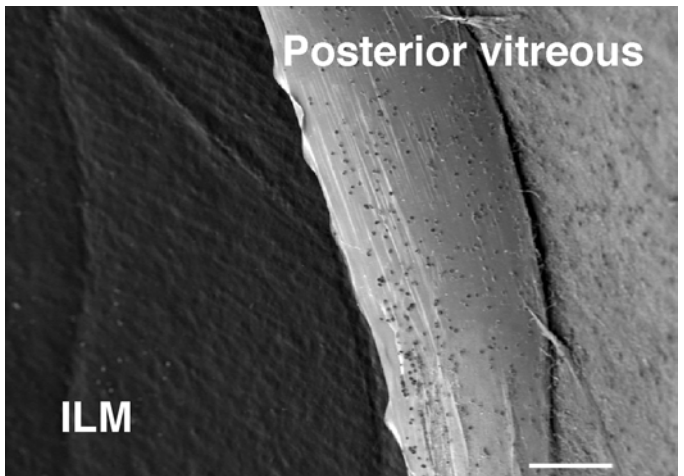
ACCEPTED MANUSCRIPT

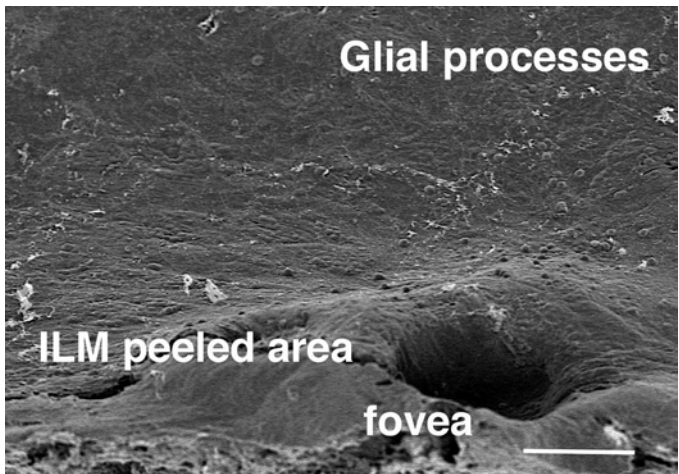


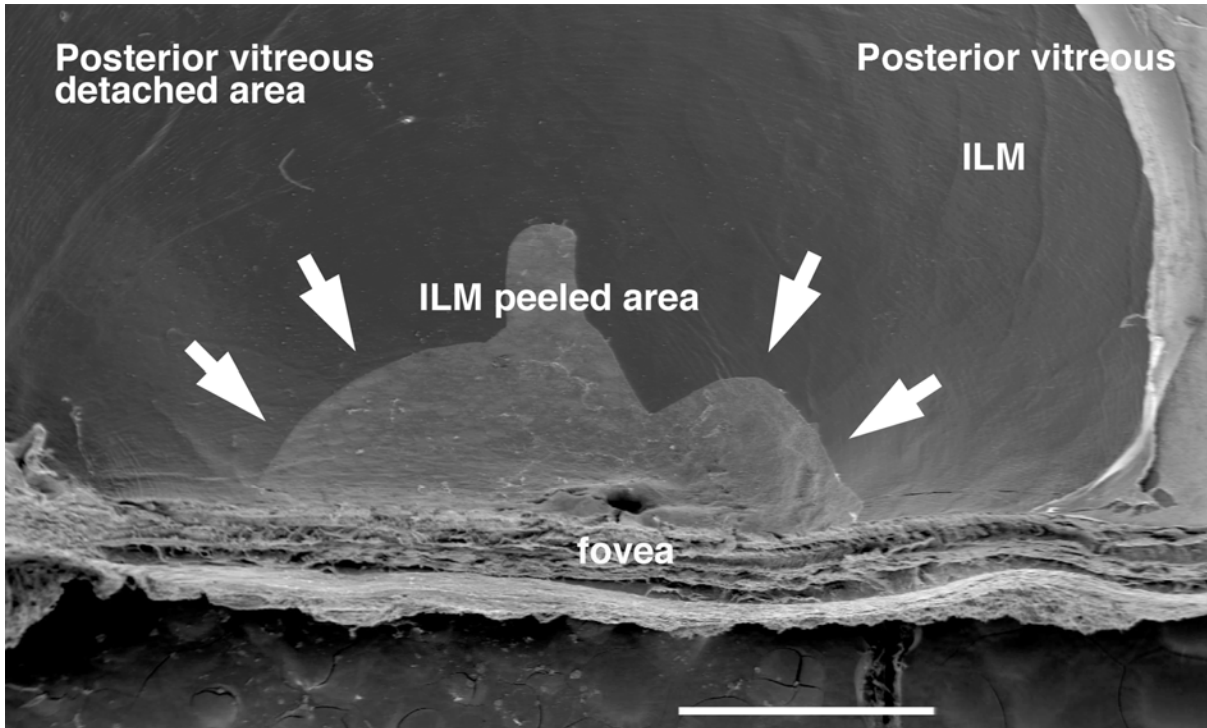
ACCEPTED MANUSCRIPT

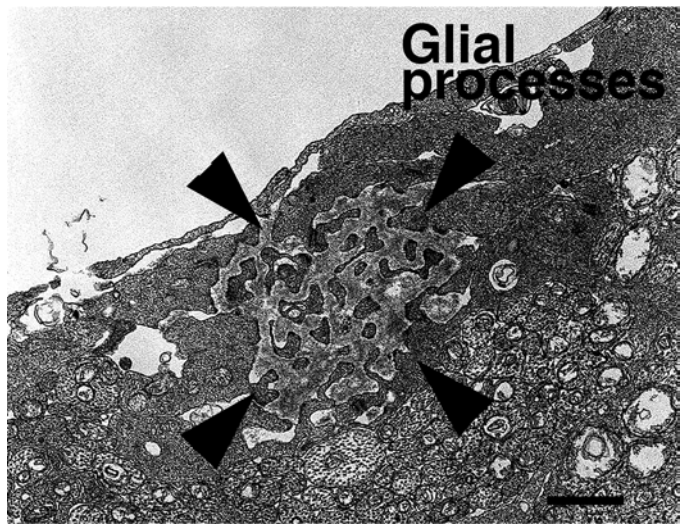


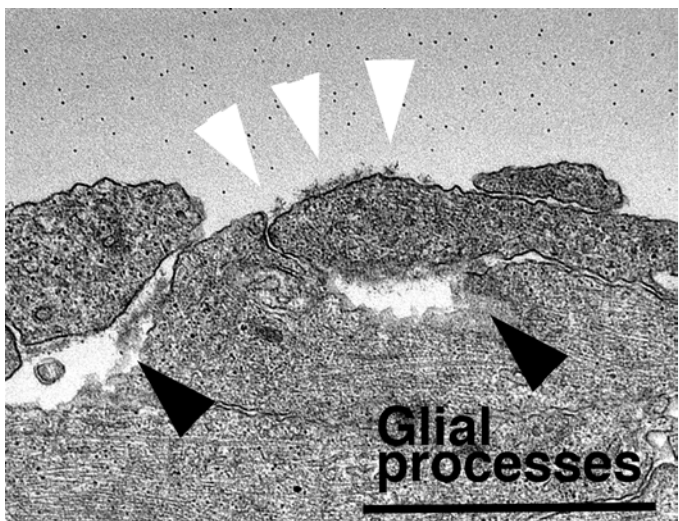


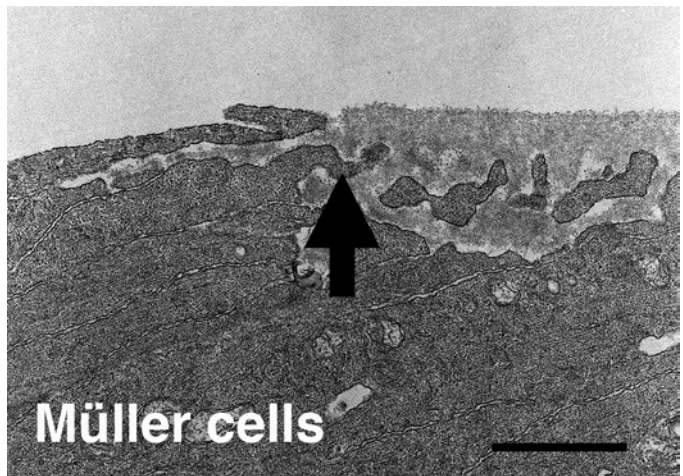


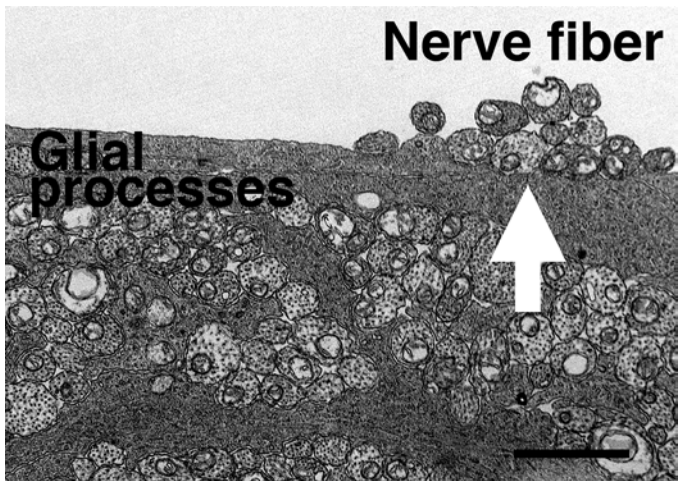


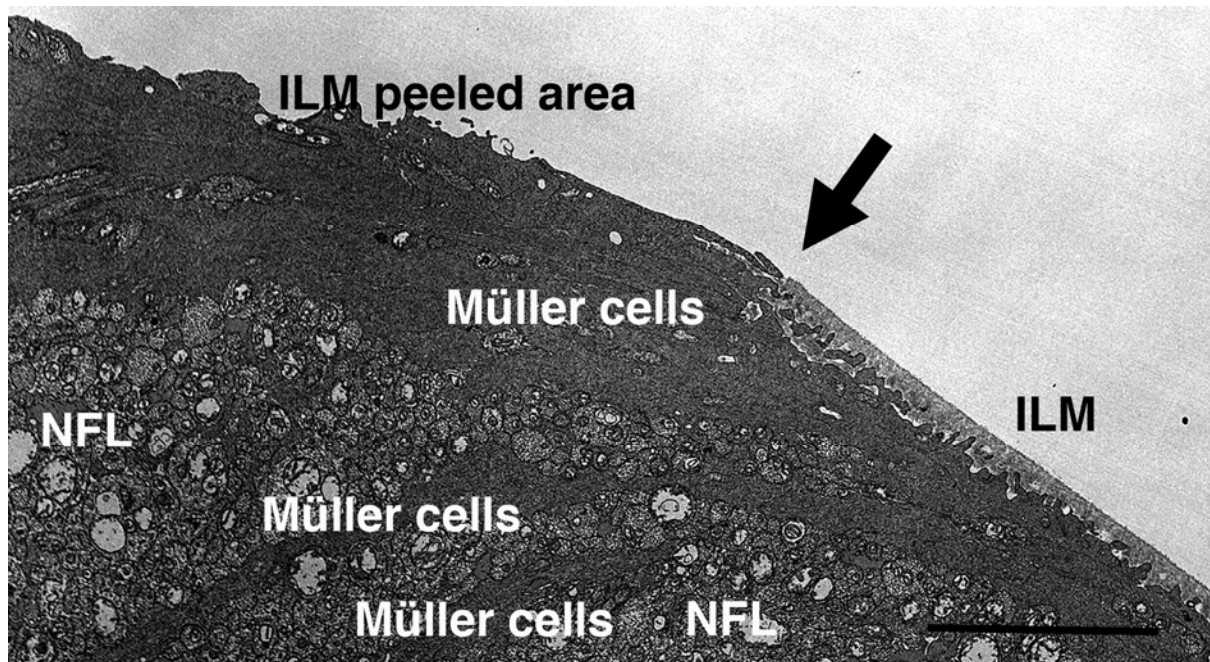












Dr. Toshio Hisatomi was a Research Associate under Dr. Joan W. Miller at Massachusetts Eye and Ear Infirmary, Harvard Medical School. He is working on the pathology of vitreoretinal interface as a vitrectomy surgeon under Dr. Tatsuro Ishibashi, Chairman of the Japanese Ophthalmological Society. His research covers wide variety of fields from clinical to basic research. He is also the inventor of an ocular staining dye, Brilliant Blue G, which is now used in chromovitrectomy.



ACCEPTED MANUSCRIPT